Cell, Vol. 49, 643-650, June 5, 1987, Copyright © 1987 by Cell Press

The Proton Flux through the Bacterial Flagellar Motor

Markus Meister,* Graeme Lowe, and Howard C. Berg
Department of Cellular and Developmental Biology
Harvard University
Cambridge, Massachusetts 02138

Summary

Bacterial flagella are driven by a rotary motor that utilizes the free energy stored in the electrochemical proton gradient across the cytoplasmic membrane to do mechanical work. The flux of protons coupled to motor rotation was measured in Streptococcus and found to be directly proportional to motor speed. This supports the hypothesis that the movement of protons through the motor is tightly coupled to the rotation of its flagellar filament. Under this assumption the efficiency of energy conversion is close to unity at the low speeds encountered in tethered cells but only a few percent at the high speeds encountered in swimming cells. This difference appears to be due to dissipation by processes internal to the motor. The efficiency at high speeds exhibits a steep temperature dependence and a sizable deuterium solvent isotope effect.

Introduction

Flagellated bacteria propel themselves through an aqueous medium by rotating helical flagellar filaments (Berg and Anderson, 1973; Berg et al., 1982; Macnab and Aizawa, 1984). A small rotary motor anchored in the cell wall at the base of the filament converts the electrochemical energy stored in the proton gradient across the cytoplasmic membrane to mechanical work. Four quantities characterize the steady-state operation of the flagellar motor: the energy consumption at the input is determined by the protonmotive force (the free energy per unit charge required to transfer protons into the cell) and the proton flux (the number of protons passing through the motor in unit time), while the rate at which mechanical work is performed at the output is determined by the torque applied to the filament (the work performed per unit angle) and the speed of rotation of the filament (the number of revolutions relative to the cell wall per unit time).

A motile species of Streptococcus has emerged as the organism of choice for physiological studies of the flagellar motor. This bacterium lacks endogenous energy reserves, so it can be starved until no metabolic protonmotive force remains. The gram-positive cell wall leaves the cytoplasmic membrane accessible to ionophores, which facilitates the generation of artificial proton gradients. Flagellar rotation can be studied by tethering a cell to a glass surface by one of its flagellar filaments, in which case the body spins about an axis through the point of attachment at rates from 0 to approximately 10 Hz. Recently it has become possible to measure the motor's rotation rate in swimming cells, and speeds up to 100 Hz have been found (in glycolyzing cells swimming at room temperature; Lowe et al., 1987). Whether a cell is tethered or swimming, the torque generated by its flagellar motors can be calculated from the viscous drag on the rotating cell body.

At the low speeds attainable by tethered cells, the torque developed by the motor is directly proportional to the protonmotive force over a wide range of values (Manson et al., 1980; Conley and Berg, 1984; Khan et al., 1985). At a fixed protonmotive force, that torque is independent of temperature and remains unaltered when cells are energized in buffers prepared with D_2O (Khan and Berg, 1983). Furthermore, the torque changes very little when the speed is reduced by the addition of viscous agents (Manson et al., 1980) or when rotation is stopped completely by external viscous flows (M. Meister and H. C. Berg, unpublished data). These observations have led to the suggestion that rotation of the flagellum is tightly coupled to proton flux, i.e., that a fixed number of protons move through the motor during each revolution, and that the efficiency of energy conversion in a tethered cell is close to unity, i.e., that all of the electrochemical free energy given up by a proton as it passes through the motor is converted to mechanical work. Under those conditions one predicts that the work per revolution, and thus the torque of the motor, is proportional to the protonmotive force but independent of temperature and hydrogen isotope, as observed.

At the high rotation rates found in swimming cells the motor generates considerably less torque. In the intermediate region, studied in swimming cells by addition of viscous agents to the medium, the torque decreases approximately as a linear function of speed (Lowe et al., 1987). If flagellar rotation is, indeed, tightly coupled to the flux of protons, then this drop in torque represents dissipation of free energy by processes internal to the motor.

Here we report measurements of the proton flux associated with rotation of the flagellar motor of Streptococcus. Cells in suspension were energized with an artificial proton gradient large enough to induce swimming. The rotation rate of the flagellar motors was inferred from the vibrational motion of the cell bodies, and the flux of protons into the cells was deduced from the rise in the pH of the external medium. Shortly after energization, antibody raised against flagellar filaments was added to the suspension. This cross-linked the filaments and stopped the rotation of the flagellar motors, causing a sudden decrease in the rate of proton uptake. That rotation-dependent component of the proton flux was found to be directly proportional to the motor's speed under a variety of conditions, lending support to the hypothesis of tight coupling. Simultaneous measurements of protonmotive force, proton flux, motor torque, and motor speed allowed an estimate of the efficiency of energy conversion in the motor,

* Present address: Department of Neurobiology, Stanford University School of Medicine, Stanford, California 94305.

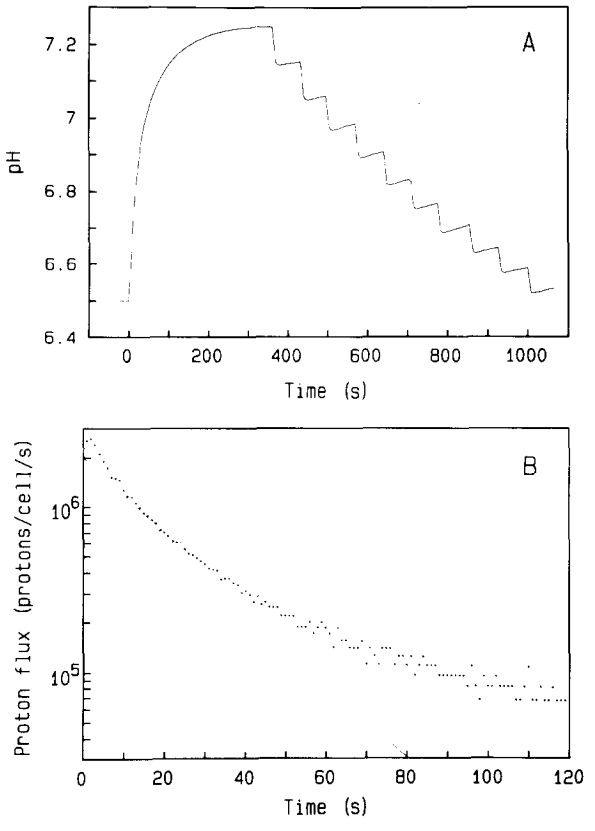

Figure 1. The Time Course of Proton Uptake following Energization

(A) The pH of the cell suspension as a function of time after energization under standard conditions. Starting at approximately 6 min after dilution, small aliquots of HCl were added to the suspension to titrate it back to the initial pH.

(B) The proton flux per cell, calculated from the data in (A), is shown as a function of time on a semilogarithmic scale. The solid line is a least-squares exponential fit to the proton flux over the time interval from 15 to 25 sec.

which proved to be close to unity at the speeds of tethered cells but only a few percent at the speeds found in swimming cells. In the latter case, the efficiency increased with temperature and decreased when the cells were energized in D_2O. Mechanisms that might account for these changes are discussed.

Results

The rotation-dependent proton flux was obtained as the difference between two measurements of the total proton flux made on the same set of cells in rapid succession. During the first measurement, the flagellar motors were rotating; in the second, they were stopped. Since the protonmotive force serves as an energy source for other processes, such as ATP synthesis and active transport, and since the membrane might contain nonspecific leaks to protons, it is possible that only a small portion of the total proton flux passes through the flagellar motor. In order to resolve this component reliably we needed to find experimental conditions that maximized the rotation rate of the motor and minimized the total proton flux. These preliminary studies are documented elsewhere (Meister, 1987). The final measurements of the rotation-dependent proton flux are described below.

Proton Movements following Artificial Energization

To ensure that the cells swam smoothly without tumbling, we used the mutant SM197, which rotates its flagella exclusively counterclockwise (Berg et al., 1982). Vigorous swimming motility required that both a pH gradient and an electric field be applied across the cell membrane. Cells that had been pretreated with the potassium ionophore valinomycin were suspended at pH 8.5 in a buffer containing 0.2 M KCl and then diluted 40-fold into a second buffer at pH 6.5 that did not contain potassium. Thus the cell membranes were subjected both to a pH difference and to a potassium diffusion potential, oriented so as to drive protons into the cytoplasm. Uptake of protons by the cells caused the pH of the medium to rise, as shown in Figure 1A. At approximately 5 min after energization, transmembrane proton movement had ceased. Subsequently, the cell suspension was titrated back to its initial pH with aliquots of HCl, which provided a measure of the buffering capacity of the external medium. The proton flux per cell was deduced from the rate of change of the external pH, the external buffering capacity, and the cell density of the suspension, as described in Experimental Procedures. Figure 1B shows a semilogarithmic plot of the rate of proton uptake as a function of time after energization, calculated from the raw data in Figure 1A. Note that the measurement was perturbed for the first 5 to 10 sec by mixing artifacts. Within the first minute the proton flux decayed with a roughly exponential time course. An exponential fit over the interval from 15 to 25 sec after energization extrapolates to an initial proton influx of $(2.0 \pm 0.1) \times 10^6$ protons per cell per second and a time constant for 10-fold decay of (44 ± 2) sec. At later times the decay occurred somewhat more slowly. This time course was reproducible to within 2% to 3% in successive samples of cells taken from the same stock suspension. However, the values of the initial flux and of the decay time varied with a standard deviation of 8% in experiments performed on cells from different cultures.

The decay in proton flux is expected, given that acidification of the cytoplasm and alkalinization of the external medium decrease the pH gradient, while movement of potassium from the inside to the outside of the cell, required for charge balance, decreases the diffusion potential. However, the initial rate of decay was much more rapid than expected from measurements of motility, made either on swimming cells or with tethered cells energized in an identical fashion. About 81% of the cells showed vigorous swimming motility for the first minute after dilution and thus appeared to retain a significant protonmotive force over a time period in which the rate of proton uptake dropped by a factor of 10 (Figure 1B). The remaining 19% of the cells, if assumed to have leaky membranes, were too few to account for the large initial proton movements. Even these cells swam vigorously on addition of 0.01 M of

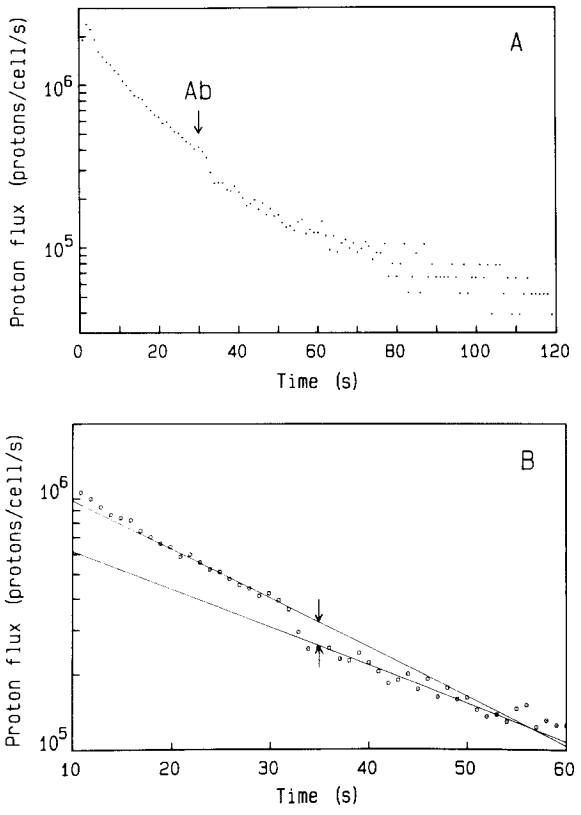

Figure 2. The Effects of Flagellar Antibody on the Rate of Proton Uptake

(A) The total proton flux following energization under standard conditions. At 30 sec after energization, 20 μl of antibody stock was added to the sample, as indicated by Ab.

(B) A segment of the data shown in (A). The upper solid line is a least-squares exponential fit to the proton flux over the interval from 20 to 30 sec, and the lower line is a similar fit over the interval from 35 to 45 sec. The arrows indicate the flux change attributed to the addition of flagellar antibody.

glucose (see below). The speed of the tethered cells decreased by only 20% over the first minute after dilution. These observations suggest that a significant protonmotive force remained even when proton movement had virtually ceased. The reasons for this behavior are not known.

Measurement of the Rotation-Dependent Flux

In our first attempts to measure the flux of protons through the flagellar motor we followed the proton movements in two successive samples of cells taken from the same stock, one of which was pretreated with flagellar antibody. In each case the initial proton flux was deduced from exponential extrapolation, as shown in Figure 1B. No significant difference was found in comparing the values obtained from the two samples. It is now clear that the rotation-dependent component was smaller than the reproducibility of the measurement of the initial flux in separate samples handled identically.

The resolution of the rotation-dependent flux improved greatly when we added flagellar antibody to the suspension of swimming cells 30 sec after energization. The antibody suppressed all swimming motility within the time required for mixing of the sample. The corresponding rate of proton uptake is shown in Figure 2A. Within 3 to 5 sec after the addition of antibody the proton flux dropped abruptly, then resumed its gradual decay. The magnitude of the discontinuity in flux was determined from the two exponential fits shown in Figure 2B, as described in Experimental Procedures. The success of this method lies in the fact that the total proton flux has decayed appreciably at the time of antibody addition and in the elimination of errors resulting from the use of two separate samples, particularly the uncertainties in the buffering capacities and cell densities of the two suspensions.

Several tests were undertaken to ascertain that this drop in the proton flux was due to the suppression of flagellar rotation. The external buffering capacity of the cell suspension increased by at most 2% on addition of antibody, so this could not account for the 20% decrease in the rate of pH change evident in Figure 2B. To test for the possibility that aggregation of cells in tight clumps might limit the diffusive flux of protons through the weakly buffered medium to the cell surface, we repeated the experiments with the flagellated but nonmotile Streptococcus mutant V4058 (derived from the wild type, V4051, following mutagenesis with ethyl methanesulfonate) and found no significant drop in the proton flux on addition of antibody. Finally, cells of strain SM197 that had been pretreated with antibody showed no suppression of proton flux when antibody was added following energization.

Three corrections were applied in order to determine the rotation-dependent proton flux associated with each flagellar motor. Even at low concentrations of antibody, swimming was completely inhibited, but many cells still showed nonrandom motion. Presumably, some flagellar rotation persisted, although formation of a bundle was blocked by the cross-linking of a few filaments. Therefore, we studied the dependence of the antibody-dependent change in flux on the concentration of the antibody. We found an approximately hyperbolic relationship, with half-maximal suppression of the proton flux when 14 μl of antibody stock was added to the 2 ml sample (Meister, 1987). To extrapolate to total inhibition of flagellar rotation, the antibody-dependent change in flux was multiplied by (v + 14 μl)/v, where v denotes the volume of antibody stock added.

We also took into account the fact that about 19% of the cells failed to swim prior to addition of the antibody, although most of them showed some motility. This was not caused by a paucity of flagella or the breakage of filaments during the washing procedure, since virtually all of the cells swam vigorously if 0.01 M of glucose was added to the suspension. Presumably, the motors of cells that did not swim during the flux measurement rotated too slowly to allow formation of a bundle. Therefore, we assumed that they did not contribute to the rotation-dependent change in flux and corrected that value accordingly.

Finally, we computed the rotation-dependent flux per

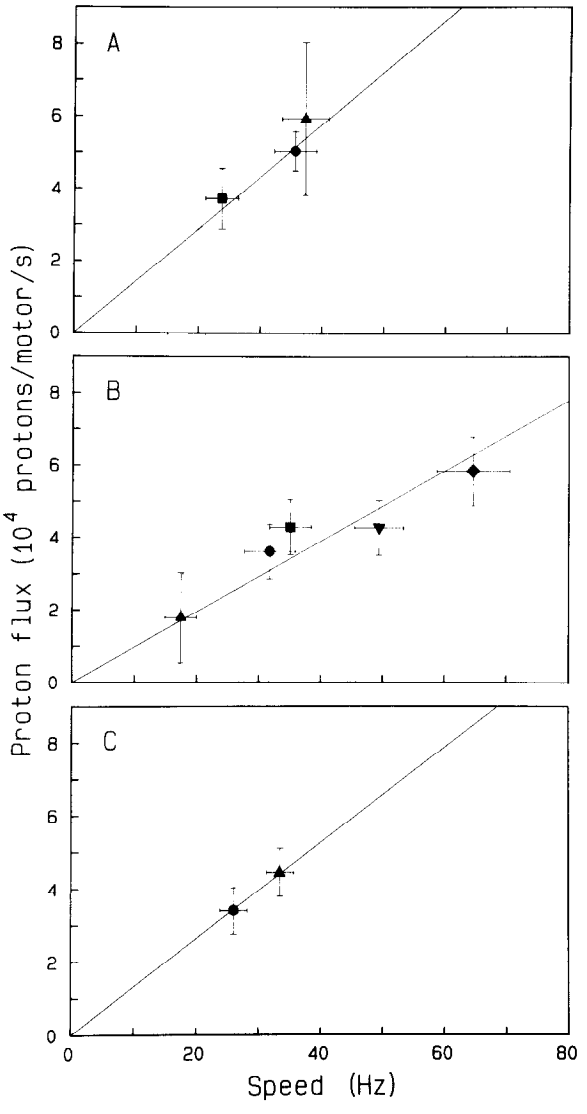

Figure 3. The Rotation-Dependent Proton Flux as a Function of Motor Speed

The speed of the motor was varied by changing (A) the time between energization and the measurement of rotation-dependent flux (▲, 22 sec; ●, 35 sec; ■, 48 sec); (B) the temperature of the energization buffer (▲, 16°C; ●, 20°C; ■, 24°C; ▼, 28°C; ◆, 32°C); and (C) the hydrogen isotope in the medium (▲, ^1H; ●, ^2H).

The solid lines are linear least-squares fits constrained through the origin and weighted with the experimental errors in the flux measurements.

motor by dividing the value for the flux per cell, corrected as described above, by the mean number of filaments per cell. This number, 3.3, was determined by flagellar staining in wet mounts, as described in Experimental Procedures.

The Relationship between Rotation-Dependent Proton Flux and Motor Speed

In order to investigate the coupling between proton flow and motor rotation, we measured the rotation-dependent proton flux at various motor speeds. The motility of cells withdrawn from the energized sample was monitored on video tape under phase-contrast microscopy. Swimming speeds were determined from the video record, and the corresponding flagellar rotation rates were inferred using the ratio of rotation rate to swimming speed measured with glycolyzing cells, as described in Experimental Procedures.

The rotation rate of the motor decreased with time after energization, presumably because of the decay in protonmotive force. Figure 3A shows the rotation-dependent proton flux as a function of motor speed, measured at successively larger times after energization. The speed dropped by approximately 35% between 22 sec and 48 sec after energization, and there was a parallel decrease in the rotation-dependent flux. Note that the total proton flux across the membrane decreased by more than a factor of 3 over the same period (Figure 1B).

In swimming cells the rate of flagellar rotation increased markedly with temperature (as seen earlier in glycolyzing cells by Lowe et al., 1987). Figure 3B shows the relationship between rotation-dependent proton flux and motor speed when measured at various temperatures. The speed increased by about a factor of 3 from 16°C to 32°C, and there was a parallel increase in the rotation-dependent flux.

Finally, we found that the motors spun 22% more slowly when driven by deuterons than when driven by protons. As shown in Figure 3C, the rotation-dependent flux changed by a similar fraction.

Thus under all conditions tested, we found that the rotation-dependent flux of protons varied proportionally to the rotation rate of the motor. From the slope of the linear fits in Figures 3A, 3B, and 3C, the ratio of rotation-dependent flux to motor speed was found as (1440 ± 130) protons per revolution, (970 ± 90) protons per revolution, and (1310 ± 150) protons per revolution, respectively. Each of the three experiments was performed with cells from a different culture. We attribute the discrepancies among the above ratios of flux to speed to variability among these cultures, for example, in the mean number of motors per cell, which was not determined for each separate experiment. On average over these three studies the ratio of the rotation-dependent flux to the motor speed was (1240 ± 240) protons per revolution.

The Relationship between Motor Torque and Motor Speed

A measurement of the motor's torque is required to estimate its power output. Earlier studies on glycolyzing Streptococcus (Lowe et al., 1987) showed that the flagella of swimming cells generate a relatively low torque but spin at a high speed, within 10% of the zero-load speed (the speed at vanishing torque, observed when the motor spins a free proximal hook). Tethered cells, on the other hand, rotate very slowly, but their torque is comparatively large and close to the motor's stall torque (the torque at vanishing speed; M. Meister and H. C. Berg, unpublished data). To obtain these two extremes of the torque-speed relationship we energized tethered cells with the same

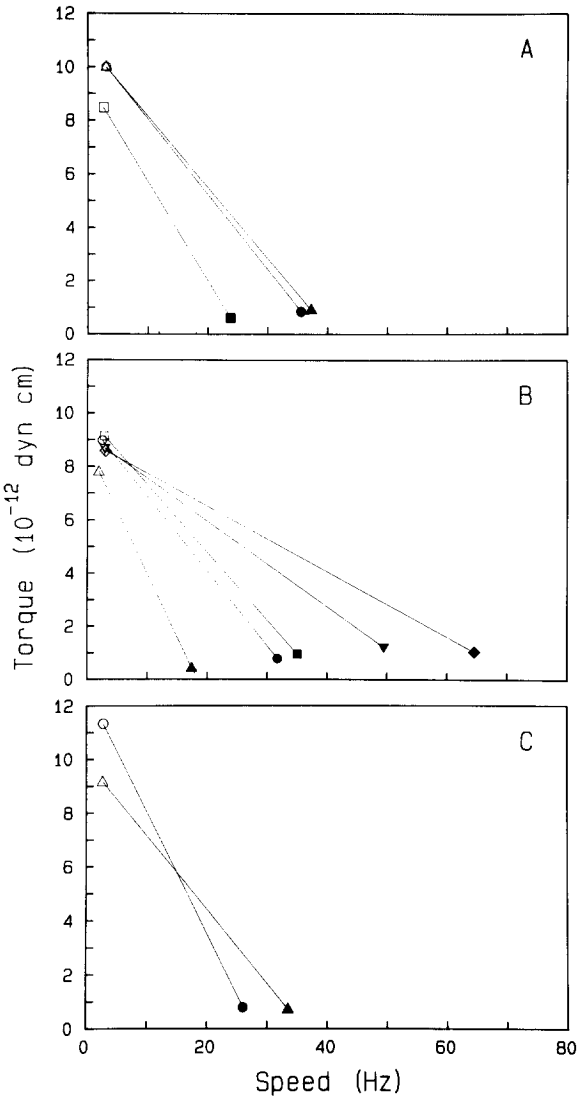

Figure 4. The Torque of the Flagellar Motor as a Function of Speed

The speed of the motor was varied by changing (A) the time between energization and measurement, (B) the temperature, and (C) the hydrogen isotope. The data are plotted with symbols defined in the legend to Figure 3. For each set of energization conditions, speed and torque were determined in both tethered cells (open symbols) and swimming cells (closed symbols). Each pair of data points is connected by a solid line for identification.

protocol applied to swimming cells during the flux measurements. In both cases, we calculated the torque from the rotation of the cell body relative to the surrounding medium, as described in Experimental Procedures.

Figure 4A shows a graph of torque as a function of speed when measured at various times after energization. For each time value the plot contains two data points, one taken from tethered cells, the other from swimming cells. They are connected by a line merely for identification. A plot of torque against speed when measured at various temperatures is shown in Figure 4B. The graph in Figure 4C compares motor torque and speed when measured in H_2O buffers and in D_2O buffers.

Under all conditions tested, the torque generated by tethered cells dramatically exceeded the value measured in swimming cells.

Discussion

We have found that the change in the transmembrane proton flux associated with the suppression of flagellar rotation is directly proportional to the motor's rotation rate over a wide range of conditions. This suggests that the motor's mechanism might link proton flow to the rotation of the filament in a constant ratio, much as the wheels in a gear box link the revolutions of input and output shafts. In that case, no protons could traverse a stalled motor, and thus the rotation-dependent component of the transmembrane proton flux would constitute the entire flux of protons through the flagellar motor. In principle, one can conceive of motor mechanisms that show a nonvanishing leakage flux at stall, in which case the total flux through the motor might greatly exceed the rotation-dependent component. By ad hoc construction, one might accommodate the result that the flux through the motor increases by an amount that is proportional to speed, and that the proportionality constant is independent of temperature and of the hydrogen isotope. However, the assumption of tight coupling between proton movement and flagellar rotation provides the simplest explanation of our observations, and it will serve as a working hypothesis for the following discussion (for further treatment of alternative coupling mechanisms, see Meister, 1987).

An important consistency check of this hypothesis is provided by an analysis of the motor's behavior at very low speeds. When the motor is stalled by an externally applied torque, no mechanical work is performed. Under the assumption of tight coupling, the proton flux through the motor also vanishes, so no energy is consumed at the input. Since no dissipation of energy occurs in the stalled motor, the power consumed at the input at infinitesimally small rotation rates must equal the power produced at the output. Thus the efficiency of energy conversion approaches unity as the motor's speed approaches zero:

$$\text{(efficiency)} = \frac{2\pi \times \text{(torque)} \times \text{(rotation rate)}}{e \times \text{(protonmotive force)} \times \text{(proton flux)}} \quad (1)$$

$$\rightarrow 1 \text{ at stall,}$$

where e is the electronic charge.

To test this prediction, we computed the efficiency of energy conversion in tethered glycolyzing cells. On average, these cells generated a torque of 2.2×10^{-11} dyn cm (determined as described in Experimental Procedures), a value close to the stall torque. A metabolically generated protonmotive force of approximately −150 mV has been reported under similar conditions in Streptococcus lactis (Kashket, 1985), and we used this value in our calculations. Under the assumption of tight coupling, the ratio of proton flux to rotation rate is equal to 1240 protons per

revolution and is independent of motor speed. Substituting these quantities in Equation 1, one calculates an efficiency of energy conversion of 0.5. An independent estimate was obtained from the measurements on tethered cells reported by Conley and Berg (1984). These cells were energized with small membrane potentials, and their speed was roughly proportional to the protonmotive force. By calculating the corresponding torque and assuming the same ratio of proton flux to rotation rate (1240 protons per revolution), one finds a value of 0.9 for the efficiency of energy conversion. These estimates are affected by numerous experimental uncertainties, including errors in the rotation-dependent proton flux, the motor speed in swimming cells, the number of motors per cell, the calculations of torque, and the estimate of protonmotive force. Nevertheless, we are confident that our result is accurate to within a factor of 2. Thus the efficiency of torque generation at very low speeds lies within the experimental resolution of unity, which is consistent with the hypothesis of tight coupling.

By the same method, we calculated the efficiency of energy conversion in glycolyzing swimming cells as 0.05. Earlier experiments have shown that the decrease in torque at high speeds is not caused by friction within the flagellar bundle. For example, wild-type cells of Escherichia coli spin their flagellar bundles at nearly the same speed as mutants without filaments (*hag* mutants) spin their free proximal hooks (cf. Lowe et al., 1987). If the motor couples proton flow and rotation of the filament in a constant stoichiometric ratio, then the decrease in efficiency at higher speeds must result from power dissipation internal to the motor mechanism. Some clues as to the processes contributing to this dissipation can be gained from the measurements of torque and speed at various temperatures and in D_2O buffers. Figure 4B shows that the stall torque is relatively invariant with temperature, confirming the observations of Khan and Berg (1983); the zero-load speed, on the other hand, increases markedly at higher temperatures. Whatever process dominates the dissipation of power in the motor, and thus limits the zero-load speed, is thermally activated. In D_2O we measured a larger stall torque than in H_2O (Figure 4C), in apparent contradiction to the results of Khan and Berg (1983), who saw no significant difference. However, it is possible that the protonmotive force was larger during our measurements in D_2O than in H_2O. For example, the total proton conductance of the membrane was larger in H_2O, which might have caused greater decay of the protonmotive force during the time between energization and the speed measurements. Nevertheless, the zero-load speed of the motor was lower in D_2O buffers (Figure 4C), pointing to a significant isotope effect. Whether this is a primary or secondary isotope effect is not yet known. It is possible that the processes that limit the zero-load speed involve proton transfer. In particular, the conduction of protons along chains of ligands, which would involve repeated breaking of weak bonds, might exhibit both the thermal activation and the isotope effect observed for the motor's zero-load speed. Such chains might serve as channels that conduct protons to the site of mechanical coupling, as in a model of the flagellar motor proposed by Berg and Khan (1983), or they might themselves be part of the active machinery, as in a mechanism proposed by Läuger (1977).

To date, all available evidence regarding the function of the flagellar motor is consistent with the hypothesis of tight coupling. If this assumption is correct, then little else can be learned from the steady-state rotation of tethered cells, which up to now has been the focus of most studies of the dynamics of flagellar rotation. The motors of these cells spin close to the stall torque, which, as seen from Equation 1, is determined solely by the protonmotive force and the coupling ratio of protons to revolutions. However, at the high speeds of operation encountered in swimming cells, the torque decreases because of dissipation within the motor. Studies of flagellar rotation in this high-speed regime can yield more information on the processes involved in torque generation and thus merit further attention.

Experimental Procedures

Materials

2-(N-morpholino)ethane sulfonic acid (MES, pK_a = 6.1), tris (hydroxymethyl)methylaminopropanesulfonic acid (TAPS, pK_a = 8.4), choline chloride, choline base, valinomycin, N,N'-dicyclohexylcarbodiimide (DCCD), and tannic acid were obtained from Sigma. Crystal violet was purchased from MCB Manufacturing Chemists, and paraffin oil from the J. T. Baker Chemical Co. Tetraethylenepentamine (tetren) was recrystallized by the method of Reilly and Vavoulis (1959) from a technical-grade product supplied by Aldrich. Flagellar antibodies were raised by injecting rabbits with fragments of Streptococcus V4051 flagellar filaments in the presence of Freund's complete adjuvant. The IgG fraction of the immune serum was purified by ammonium sulfate fractionation and DEAE chromatography. Dialysis against 0.067 M $MgCl_2$, 0.1 mM tetren at pH 7 yielded the stock solution used during flux measurements. Other chemicals were of reagent grade.

Energization Conditions

Initiation of swimming in artificially energized cells requires a protonmotive force of −80 to −100 mV (Manson et al., 1977; Matsuura et al., 1979), significantly larger than the threshold for rotation of tethered cells (Manson et al., 1980; Conley and Berg, 1984; Khan et al., 1985). The magnitude of the pH shift during energization is limited technically by deleterious effects on flagellar motility of pH values above 9 or below 6. Also, one cannot dilute the potassium concentration by much more than a factor of 100 without raising the cell density in the stock suspension beyond a practical limit or impairing the flux measurement in an overly dilute final sample. Under these constraints, a combination of pH gradient and membrane potential was required to sustain vigorous swimming motility over the first minute after energization.

The media chosen for energization were buffered with MES and TAPS to avoid complications that might arise from transport of inorganic phosphate. Magnesium, rather than sodium, was used to maintain the ionic strength on dilution of potassium, because the possibility of Na^+/H^+ exchange complicates the interpretation of proton movements. Tetren, which has a relatively low affinity for Mg^{++}, was used to chelate the heavy metals that inhibit motility (Adler and Templeton, 1967).

An attempt to use choline to maintain the ionic strength on dilution of potassium proved unsuccessful. For unknown reasons, all motility ceased within 1 min after cells were energized with a combined pH shift and potassium dilution in choline. This effect was studied further with tethered cells, where quantitative observation of flagellar rotation is easier. In the presence of choline these cells slowed down gradually over approximately 10 min after either a 1:100 dilution of potassium or a shift from pH 8.5 to pH 6.5, but when the two were combined, the cells stopped rotating within 1 to 2 min. At that point motility recovered within

1 min when either sodium or magnesium was substituted for choline in the external medium (Meister, 1987).

Preparation of Cells

Cells of the smooth-swimming Streptococcus strain SM197 (Berg et al., 1982) were incubated at 35°C in KTY medium (Harold and Papineau, 1972) and harvested during the late exponential growth phase at a density of approximately 4×10^8 cells/ml. They were washed twice with buffer A (10 mM MES, 10 mM TAPS, 0.1 mM tetren, 0.2 M KCl; pH 8.5) by centrifugation at 4000 g for 2 min. Subsequently, valinomycin was added to the cell suspension at a concentration of 5 μg/ml. After 2 min, cells intended for flux measurements were washed twice in buffer B (1 mM MES, 1 mM TAPS, 0.1 mM tetren, 0.2 M KCl; pH 8.5). The final stock suspension had a density of 2×10^{10} to 4×10^{10} cells/ml and was kept on ice. Cells used in tethering experiments were washed in buffer A, sheared, washed again, and tethered to silanized glass cover slips, as described previously (Manson et al., 1980). At the time of measurement of proton flux or motor speed, these cells showed no sign of any residual protonmotive force: no transmembrane proton movement was observed in the stock suspension, and tethered cells did not rotate.

Proton Flux Measurements

A 2 ml volume of the energization buffer C (0.1 mM MES, 0.1 mM TAPS, 0.1 mM tetren, 0.067 M $MgCl_2$; pH 6.5 or pD 7.0; see below) was stirred vigorously in a glass vial that was thermostatted to within 0.1°C. A combination electrode (Radiometer GK2321C) was inserted in the solution, and the output signal of the pH meter (Radiometer PHM26, 10 mV/pH) was amplified and sampled at 50 millisec intervals by an Apple II microcomputer via a 12 bit A/D converter (Metrabyte APM-08). A 5 mm thick layer of paraffin oil on the surface of the sample inhibited exchange of CO_2 with the room air, which otherwise caused significant pH drifts. The flux measurement was initiated by dilution of 50 μl of cell stock suspension in the stirred energization buffer. To offset a rapid pH shift resulting from titration of species in the buffer and the cell wall, small amounts of HCl or KOH were added along with the cells. This avoided perturbations of the proton uptake recordings due to the slow response of the pH electrode. At approximately 5 min after energization, the suspension was titrated back to its initial pH by addition of a series of equal aliquots of HCl. The pH changes observed during one such experiment are shown in Figure 1A. Then the optical density of the cell suspension was measured at 600 nm (Perkin-Elmer 552 spectrophotometer with microcuvette). The ratio of OD_{600} and cell density was determined for each culture using a Petroff-Hausser bacteria counter.

The rapid downward shifts in pH following addition of acid during the titration of the cell suspension were used to determine the buffering capacity of the extracellular medium, as described by Maloney (1979). About 20% to 30% of this buffering capacity was due to the cell wall. As seen from Figure 1A, the buffering capacity decreased at high pH, thus improving the resolution of the relatively slow proton uptake at late times after energization. We interpolated the dependence of the buffering capacity on the pH with a quadratic polynomial. The recorded pH values were averaged over 1 sec intervals. The proton uptake per cell was computed for successive 1 sec intervals from the change in the pH, the external buffering capacity, and the number of cells in the sample. Figure 1B shows a semilogarithmic plot of the proton flux as a function of time after energization. Since the first 5 to 10 sec of the measurement were perturbed by mixing artifacts, we estimated the initial value of the proton flux by exponential extrapolation from the time interval between 15 and 25 sec after energization. This numerical fit also yielded an estimate of the time required for 10-fold decay of the proton flux.

Unless indicated otherwise, the energization buffer was prepared with H_2O and thermostatted at 24°C. These conditions applied during the experiment illustrated in Figure 1. When prepared with D_2O, buffer C was adjusted to pD 7.0, determined by adding 0.4 units to the reading obtained with a glass combination electrode (cf. Gandour and Schowen, 1978). Upon energization, intracellular H_2O is rapidly exchanged for D_2O. We assumed that the internal pD immediately following dilution was approximately 0.5 units higher than the internal pH prior to dilution, as observed in cells starved at pH 7.5 by Khan and Berg (1983). Thus cells diluted from buffer B at pH 8.5 to buffer C at pD 7.0 should experience an initial transmembrane deuteron gradient of 2 pD units.

In measurements of the rotation-dependent proton flux, 20 to 40 μl of antibody stock were added to the sample at 30 sec after energization (except where indicated otherwise), which led to a rapid decrease of the proton flux, as shown in Figure 2A. The analysis of these experiments is illustrated in Figure 2B. One exponential fit was made to the time course of the proton flux over an interval of 10 sec just preceding the addition of antibody. The next 5 sec of data were ignored to allow for mixing of the antibody and suppression of flagellar rotation. A second exponential fit was made over the interval from 5 to 15 sec after addition of antibody. The difference between the values predicted by these fits for the flux at the beginning of the latter interval constituted the drop in the proton flux caused by addition of antibody. This value required some correction for the fact that the proton flux did not exactly follow a simple exponential time course, which introduced some error in the extrapolation across the mixing time provided by the first exponential fit. Therefore, for each set of energization conditions, an additional measurement was performed without addition of antibody and analyzed in the same fashion. Because of the curvature seen in the semilogarithmic plot of Figure 1B, this measurement resulted in a finite difference between the two exponential fits, which was subtracted from the result of the measurement with antibody. Additional corrections to the rotation-dependent flux for its variation with the antibody concentration and the fact that some cells failed to swim are described in the text.

Finally, the rotation-dependent proton flux per cell, corrected as described above, was divided by the number of flagellar filaments per cell to obtain the rotation-dependent flux per motor. The flagellar filaments were visualized by a modified Ryu stain in a wet mount, as described by Heimbrook et al. (1986), which avoided most of the flagellar breakage that we encountered with the classic Leifson stain (Leifson, 1951). We counted between zero and seven filaments per cell, with about half of the cells showing two or three flagella. Four different cultures were examined and the mean number of filaments per cell was found to be 3.3 ± 0.3.

Speed Measurements

The method of Lowe et al. (1987), which optically detects the small vibrations of the cell body caused by an imbalance of the forces exerted on the flagellar bundle, is impractical for measuring the motor rotation frequency in artificially energized cells, because their motility does not last long enough for sufficient accumulation of data. Therefore, we deduced the rotation rate of the flagellar motor during a flux measurement from the cell's swimming speed. Since the fluid flows involved in bacterial motility are dominated by viscous forces, one expects the ratio between the rotation rate of the flagellar motors and the swimming speed of a cell to be a constant that depends only on the geometry of the cell. We verified that prediction by measuring both the motor rotation rate and the swimming speed of glycolyzing cells at various temperatures. The proportionality constant found during these experiments was then used to calculate the motor rotation rate from the swimming speed observed for artificially energized cells, as described below.

To determine the ratio of motor rotation rate and swimming speed of glycolyzing cells, a suspension of approximately 5×10^8 cells/ml in buffer A containing 0.01 M of glucose at pH 7.5 was drawn into a thermostatted flow chamber (Berg and Block, 1984) and observed by phase-contrast microscopy. The mean bundle frequency was determined from the power spectrum of vibrations of the cell bodies as described by Lowe et al. (1987). A beam splitter allowed for simultaneous recording of the swimming motility on video tape. During playback we determined the average swimming speed by tracing the paths of 20 to 30 cells on the video monitor. We also measured the rotation rates of the cell bodies by counting the wobbles exhibited by their images. The mean body-roll frequency was added to the mean bundle frequency to yield the motor rotation rate. As the temperature was varied from 12°C to 24°C, the rotation rate increased from 30 to 93 Hz. The ratio of rotation rate to swimming speed remained constant at $(6.07 \pm 0.23)\ \mu m^{-1}$.

To determine the motor rotation rates during a measurement of rotation-dependent flux, cells were artificially energized as described in the protocol for proton flux measurements. At 5 sec after dilution, the cell suspension was drawn into the flow chamber. Swimming speeds and body-roll frequencies were determined as described

above, and averaged over the 5 sec time interval corresponding to addition of antibody during a flux measurement. The mean motor rotation rate was obtained by multiplying the mean swimming speed by 6.07 μm^{-1}.

The rotation rates of tethered cells were determined by mounting the glass cover slip on a flow chamber, recording images of the cell bodies on video tape, counting their revolutions over 5 sec periods, and averaging the rotation rate over a sample of 20 to 30 cells. Glycolyzing cells were observed in buffer A with 0.01 M of glucose at pH 7.5. We also measured the rotation rates under the conditions of the proton flux measurements. Starved cells tethered in buffer A were first shifted to buffer B for several minutes. Then a suspension of energized cells was drawn into the flow chamber as described above. Thus the tethered cells experienced the same time-dependent changes in the pH and composition of the external medium as did the swimming cells during measurements of proton flux or swimming speed.

Torque Measurements

The bodies of both swimming cells and tethered cells rotate relative to the surrounding medium. In a swimming cell, the viscous rotational drag is balanced by the combined torques of all the filaments in a bundle. In a tethered cell, it is balanced by the torque of a single motor. In either case, we calculated the rotational drag coefficient of the cell body by approximating it as a cylinder and using the formulas given by Tirado and de la Torre (1979, 1980). That value was multiplied by the viscosity of the medium and the corresponding body rotation rate, obtained from video records as described above, to yield the torque exerted by the fluid on the cell body. For swimming cells, we divided this quantity by the mean number of flagella per cell to obtain the mean torque per motor. For further details on these calculations, see Lowe et al. (1987).

Acknowledgments

We thank Shahid Khan and David Blair for valuable discussions and Bob Macnab for examining the flagellation of SM197 by high-intensity light microscopy. This work was carried out in the Division of Biology at the California Institute of Technology and supported by grants from the U.S. National Science Foundation (DMB8518257) and the Gustavus and Louise Pfeiffer Foundation. M. M. and G. L. were recipients of Earle C. Anthony Fellowships.

The costs of publication of this article were defrayed in part by the payment of page charges. This article must therefore be hereby marked "*advertisement*" in accordance with 18 U.S.C. Section 1734 solely to indicate this fact.

References

Adler, J., and Templeton, B. (1967). The effect of environmental conditions on the motility of *Escherichia coli*. J. Gen. Microbiol. *46*, 175–184.

Berg, H. C., and Anderson, R. A. (1973). Bacteria swim by rotating their flagellar filaments. Nature *245*, 380–382.

Berg, H. C., and Block, S. M. (1984). A miniature flow cell designed for rapid exchange of media under high-power microscope objectives. J. Gen. Microbiol. *130*, 2915–2920.

Berg, H. C., and Khan, S. (1983). A model for the flagellar rotary motor. In Mobility and Recognition in Cell Biology, H. Sund and C. Veeger, eds. (Berlin: de Gruyter), pp. 485–497.

Berg, H. C., Manson, M. D., and Conley, M. P. (1982). Dynamics and energetics of flagellar rotation in bacteria. Symp. Soc. Exp. Biol. *35*, 1–35.

Conley, M. P., and Berg, H. C. (1984). Chemical modification of *Streptococcus* flagellar motors. J. Bacteriol. *158*, 832–843.

Gandour, R. D., and Schowen, R. L. (1978). Transition States of Biochemical Processes (New York: Plenum Press), Chapter 6.

Harold, F. M., and Papineau, D. (1972). Cation transport and electrogenesis by *Streptococcus faecalis*. The membrane potential. J. Membr. Biol. *8*, 27–44.

Heimbrook, M. E., Wang, W. L. L., and Campbell, G. (1986). Abstracts of the Annual Meeting of the American Society for Microbiology (Washington, D. C.: American Society for Microbiology), p. 240.

Kashket, E. R. (1985). The proton motive force in bacteria: a critical assessment of methods. Ann. Rev. Microbiol. *39*, 219–242.

Khan, S., and Berg, H. C. (1983). Isotope and thermal effects in chemiosmotic coupling to the flagellar motor of Streptococcus. Cell *32*, 913–919.

Khan, S., Meister, M., and Berg, H. C. (1985). Constraints on flagellar rotation. J. Mol. Biol. *184*, 645–656.

Läuger, P. (1977). Ion transport and rotation of bacterial flagella. Nature *268*, 360–362.

Leifson, E. (1951). Staining, shape, and arrangement of bacterial flagella. J. Bacteriol. *62*, 377–389.

Lowe, G., Meister, M., and Berg, H. C. (1987). Rapid rotation of flagellar bundles in swimming bacteria. Nature *325*, 637–640.

Macnab, R. M., and Aizawa, S.-I. (1984). Bacterial motility and the bacterial flagellar motor. Ann. Rev. Biophys. Bioeng. *13*, 51–83.

Maloney, P. C. (1979). Membrane H^+-conductance of *Streptococcus lactis*. J. Bacteriol. *140*, 197–205.

Manson, M. D., Tedesco, P., Berg, H. C., Harold, F. M., and van der Drift, C. (1977). A protonmotive force drives bacterial flagella. Proc. Natl. Acad. Sci. USA *74*, 3060–3064.

Manson, M. D., Tedesco, P. M., and Berg, H. C. (1980). Energetics of flagellar rotation in bacteria. J. Mol. Biol. *138*, 541–561.

Matsuura, S., Shioi, J.-I., Imae, Y., and Iida, S. (1979). Characterization of the *Bacillus subtilis* motile system driven by an artificially created protonmotive force. J. Bacteriol. *140*, 28–36.

Meister, M. (1987). Thesis, California Institute of Technology, Pasadena, California.

Reilly, C. N., and Vavoulis, A. (1959). Tetraethylenepentamine, a selective titrant for metal ions. Analyt. Chem. *31*, 243–248.

Tirado, M. M., and de la Torre, J. G. (1979). Translational friction coefficients of rigid, symmetric top macromolecules. Application to circular cylinders. J. Chem. Phys. *71*, 2581–2587.

Tirado, M. M., and de la Torre, J. G. (1980). Rotational dynamics of rigid, symmetric top macromolecules. Application to circular cylinders. J. Chem. Phys. *73*, 1986–1993.

Note Added in Proof

The work referred to as M. Meister and H. C. Berg, unpublished data, is now in press. The stall torque of the bacterial flagellar motor. Biophys. J. (1987).